EARTHQUAKE ENGINEERING AND STRUCTURAL DYNAMICS
Earthquake Engng Struct. Dyn. 2009; **38**:805–825
Published online 12 November 2008 in Wiley InterScience (www.interscience.wiley.com). DOI: 10.1002/eqe.869

Incremental dynamic analysis with consideration of modeling uncertainties‡

Matjaz Dolsek*, †

Faculty of Civil and Geodetic Engineering, University of Ljubljana, Ljubljana SI-1000, Slovenia

SUMMARY

Incremental dynamic analysis (IDA) has been extended by introducing a set of structural models in addition to the set of ground motion records which is employed in IDA analysis in order to capture record-to-record variability. The set of structural models reflects epistemic (modeling) uncertainties, and is determined by utilizing the latin hypercube sampling (LHS) method. The effects of both aleatory and epistemic uncertainty on seismic response parameters are therefore considered in extended IDA analysis. The proposed method has been applied to an example of the four-storey-reinforced concrete frame, for which pseudo-dynamic tests were performed at the ELSA Laboratory, Ispra. The influence of epistemic uncertainty on the seismic response parameters is presented in terms of summarized IDA curves and dispersion measures. The results of extended IDA analysis are compared with the results of IDA analysis, and the sensitivity of the seismic response parameters to the input random variable using the LHS method is discussed. It is shown that epistemic uncertainty does not have significant influence on the seismic response parameters in the range far from collapse, but could have a significant influence on collapse capacity. Copyright © 2008 John Wiley & Sons, Ltd.

Received 23 July 2008; Revised 19 September 2008; Accepted 22 September 2008

KEY WORDS: extended incremental dynamic analysis; performance-based earthquake engineering; uncertainty; epistemic; aleatory; latin hypercube sampling

1. INTRODUCTION

One of the most popular methods for determining seismic response parameters is incremental dynamic analysis (IDA) proposed by Vamvatsikos and Cornell [1, 2]. It can be used to take into account the effect of the aleatory uncertainty (record-to-record variability) on the engineering

*Correspondence to: Matjaz Dolsek, Faculty of Civil and Geodetic Engineering, University of Ljubljana, Jamova 2, Ljubljana SI-1000, Slovenia.
†E-mail: mdolsek@ikpir.fgg.uni-lj.si
‡This article is based on a short paper presented at the eighth PCEE (Singapore, 2007).

Contract/grant sponsor: Slovenian Research Agency

demand parameter (EDP) through the set of ground motion records (GMR), and is used for multiple purposes. For example, many researchers have used IDA for evaluation of the seismic performance of different types of structures [3–5] for studies related to advanced intensities measures [6, 7] or damage measure [8], and for the validation of simplified procedures for the prediction of approximate IDA curves [9–12] or loss estimation methodologies [13].

In addition to the effect of aleatory uncertainty (record-to-record variability) on the EDP, which can be estimated directly through IDA analysis, it is also important to evaluate the effects of epistemic uncertainty, referring herein only to modeling uncertainty. Several researchers have performed such studies using different methods. The sensitivity of a single input variable on the seismic response parameter is the simplest approach that can be used to study the influence of modeling uncertainty [14]. Based on the results of such an analysis, first-order second-moment (FOSM) reliability analysis can be applied in order to estimate the effects of several modeling uncertainties on the structural response parameters. Among others, Haselton has used the FOSM reliability approach in order to study the effects of modeling uncertainties on the collapse capacity of reinforced concrete frames designed for a high seismic region in California [15]. Lee and Mosalam [16] have studied the sensitivity of seismic demand to possible future earthquakes for a reinforced concrete shear-wall building using the FOSM method in combination with Monte Carlo simulation, whereas Baker and Cornell [17] have used the FOSM method in combination with numerical integration for the propagation of uncertainties in probabilistic seismic loss estimation. Unfortunately, the FOSM method can become inaccurate for highly nonlinear functions [18, 19]. The alternative in such cases is Monte Carlo simulation, which is computationally extremely demanding, but has the advantage of direct incorporating modeling uncertainty into the problem. The computational effort of Monte Carlo simulation can be reduced through combining it with the response surface method [18, 19].

In this paper a slightly different approach to those mentioned above has been proposed for the evaluation of the effects of aleatory and epistemic uncertainty, and has been applied to a four-storey-reinforced concrete frame. The proposed approach combines IDA analysis [1] and the latin hypercube sampling (LHS) technique [20], which is used to define a set of structural models. These models reflect the epistemic uncertainty, whereas the set of GMR used in the IDA analysis simulates the aleatory uncertainty. The results of such analysis are the well-known IDA curves, which are determined for a set of models and not only for a best-estimate model as in the original IDA analysis. The summarized IDA curves incorporate the effects of both aleatory and epistemic uncertainty.

2. METHODOLOGY

The goal of the extended incremental dynamic analysis (extended IDA) is to consider the effects of epistemic uncertainty on the structural response parameters in addition to record-to-record variability, which in the IDA analysis is introduced through a set of GMR. In the proposed methodology, this goal is achieved by introducing a set of structural models, which reflect the epistemic uncertainty. This set of structural models has to be defined in such a way that it describes the epistemic uncertainty in the best possible manner, provided that important uncertainties are considered in the set of structural models, and that the number of structural models is reasonably low. In this case, the result of the extended IDA analysis is the EDP, which depends on the intensity

DOI: 10.1002/eqe

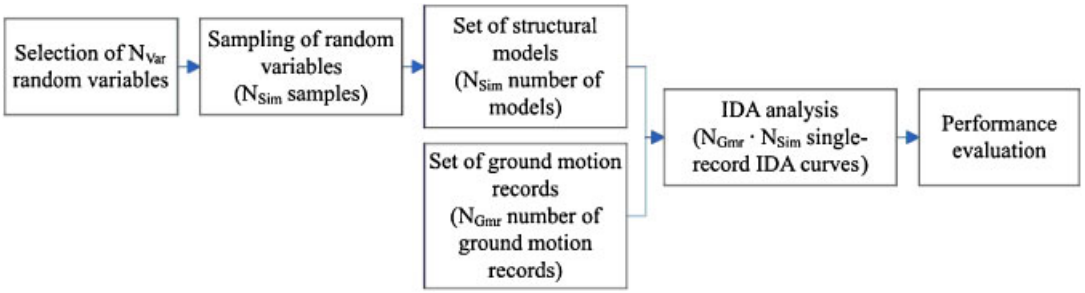

Figure 1. The main steps of the extended IDA analysis.

measure (IM), the selected set of GMR, and the selected random variables X_i, through which epistemic uncertainty is introduced into the structural models.

The main steps of the extended IDA analysis are presented in Figure 1. Extension of the IDA analysis is straightforward since the only new step in the extended IDA analysis in comparison with the IDA analysis introduced by Vamvatsikos and Cornell [1, 2] is the determination of the set of structural models. For this reason only this step will be described here. However, once the set of structural models is determined, the single-record IDA curves can be calculated for each GMR and for each structural model defined, respectively, by the set of GMR and the set of structural models. Note that exactly the same algorithms as suggested by Vamvatsikos and Cornell [1, 2] can be used to determine the single-record IDA curves. The extended IDA analysis is therefore more time consuming since the IDA curves are calculated not only for the different GMR, but also for a predefined set of structural models. However, it is still less computationally demanding than a corresponding Monte Carlo simulation.

The first step in the process of the determination of the set of structural models is the identification of the sources of epistemic uncertainty. The most common uncertainties are the mechanical characteristics of the material, the gravity loads and corresponding masses, viscous damping and effective beam width, ultimate rotations and others, which can be even more important. Basically, it is possible to include all types of epistemic uncertainties, which can be described by means of random variables. However, it is practical to consider only a limited number N_{Var} of the random variables X_i, i.e. only those that have a significant influence on the seismic response of the structure, in order to reduce the size of the set of structural models, usually referred to by the number of simulations N_{Sim}.

In the proposed methodology, the set of structural models is determined by employing the LHS [20]. It uses stratification of the probability distribution function of the random variables X_i and consequently requires significantly fewer simulations in comparison with the ordinary type of Monte Carlo simulation. In general, two steps are needed to determine the sample of random variables, which are directly applied in the structural model. First, each random variable X_i is sampled using N_{Sim} values. The most common strategy used in order to determine the samples of random variables is:

$$x_{j,i} = F_i^{-1}(p_{j,i}) = F_i^{-1}\left(\frac{j-0.5}{N_{\mathrm{Sim}}}\right), \quad i = 1, \ldots, N_{\mathrm{Var}}, \quad j = 1, \ldots, N_{\mathrm{Sim}} \tag{1}$$

DOI: 10.1002/eqe

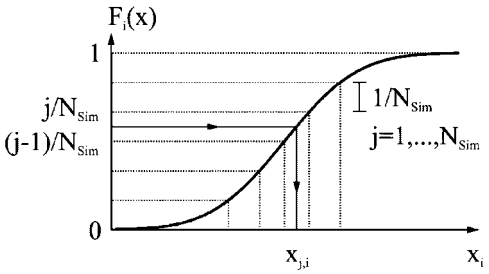

Figure 2. The sampling of random variables X_i.

where $x_{j,i}$ is the jth sample value of the ith random variable X_i, $p_{j,i}$ is the probability that the random variable X_i is less or equal to $x_{j,i}$ and $F_i^{-1}(p_{j,i})$ is the inverse of the cumulative distribution function of the random variable X_i evaluated at probability $p_{j,i}$. The probabilities $p_{j,i}$, represented by N_{Sim} equidistant points in the interval from $0.5/N_{\text{Sim}}$ to $1–0.5/N_{\text{Sim}}$, ensure that each random variable is properly sampled (Figure 2). However, during the sampling of each random variable X_i, an undesired correlation between the different random variables is usually introduced. For example, instead of having a correlation coefficient equal to the prescribed correlation coefficient between two random variables, e.g. zero if the two random variables are defined as being uncorrelated, the correlation coefficient, calculated based on the sample values (Equation (1)) of the two random variables, is actually equal to one if the distribution of the two random variables are of the same type, or close to one, if the distribution types differ. For this reason the sample values $x_{j,i}$ are not yet appropriate for the determination of the set of structural models, since the generated correlation matrix $\mathbf{S}$, which is calculated based on the sample values $x_{j,i}$, is not yet close to the prescribed (target) correlation matrix $\mathbf{K}$. Note that in the case that the equidistant interval $(j-0.5)/N_{\text{Sim}}$ (Equation (1)) is based on the random permutations, which is the usual case in the classic LHS technique, then the correlation coefficient between the sample values of the two random variables is much less than 1, and is usually close to 0 if the sample size is large. However, the difference between the two correlation matrices can be minimized by the permutation of elements of the sample matrix $\mathbf{X}$, which contains the sample values $x_{j,i}$. This represents the second step in the process of the determination of the sample of random variables. This problem can be successfully solved by the stochastic optimization method called simulated annealing [20], which was also employed in the extended IDA analysis, and is briefly described here.

First, a norm E, which is a measure for the difference between the generated and the prescribed correlation matrix, is introduced:

$$E = \frac{2}{N_{\text{Var}}(N_{\text{Var}}-1)} \sqrt{\sum_{i=1}^{N_{\text{Var}}-1} \sum_{j=i+1}^{N_{\text{Var}}} (S_{i,j} - K_{i,j})^2} \tag{2}$$

where $S_{i,j}$ and $K_{i,j}$ are, respectively, generated and prescribed correlation coefficients between the random variables X_i and X_j, and N_{Var} is the number of random variables. The norm E takes into account the deviations between all the correlation coefficients and is normalized with respect to the total number of all correlation coefficients. It therefore represents a good measure when examples with a different number of random variables are compared. The norm E is also

DOI: 10.1002/eqe

an objective function, which is minimized by continuing the two steps: mutation and selection. Mutation represents the random change of the rank of one randomly selected random variable. For example, a vector (column) from the sample matrix $\mathbf{X}$, which represents the sample of one random variable, is randomly selected and the two randomly selected ranks of the randomly selected vector are then exchanged, i.e. rank m becomes rank n and vice versa. After such a mutation, the sample matrix $\mathbf{X}$ is changed and the new norm E can be calculated. The second step, selection, decides if the new generation of the arrangement of the sample matrix $\mathbf{X}$ is acceptable or not. However, it is automatically accepted if the new arrangement of the sample matrix $\mathbf{X}$ results in a decreasing of the norm E. Otherwise, if the new arrangement does not decrease the norm E, the new arrangement is accepted if the random variable

$$Z = \mathrm{e}^{-\Delta E/T} - R \tag{3}$$

is positive, where ΔE is the difference between the norm E before and after the mutation, T is the so-called temperature and R is the uniformly distributed random variable between the interval 0 and 1. Note that the name for parameter T comes from annealing in metallurgy, which is also the reason for the name of the employed stochastic optimization method simulated annealing [20]. In our case the initial temperature T represents the maximum possible norm E (Equation (2)), which can be easily calculated from the fact that the correlation coefficients are always within the interval from -1 to 1. The maximum norm E is therefore obtained by assuming the correlation coefficient $S_{i,j}$ to be -1 and 1, respectively, if the correlation coefficient $K_{i,j}$ is negative or positive. However, after a certain number of mutations the temperature T has to be decreased by a factor, which is usually taken to be 0.95. The optimization process (mutation and selection) stops when the temperature T becomes reasonably low (e.g. 10^{-5}). The optimal number of mutations N_{m} between the two temperatures depends on the size of the optimization problem. For example, if N_{Var} is about 10 and N_{Sim} is less than 100, then a good choice for N_{m} is about 1000. The result after the optimization process is the optimized sample matrix $\mathbf{X}$ with N_{Sim} rows and N_{Var} columns, for which the correlation matrix is close to the target correlation matrix.

The set of structural models is then simply determined by employing the optimized sample matrix $\mathbf{X}$. For example, the jth structural model from the set of structural models is determined based on the sample values defined in the jth row of the optimized sample matrix $\mathbf{X}$. Since the number of rows of the sample matrix $\mathbf{X}$ is equal to N_{Sim}, the same number of structural models, which form a set of structural models, has to be generated. Note that one random variable may affect more than one parameter in the structural model. For example, if mass is simulated with a random variable, it affects not only the mass but also the vertical loading, or, if the slab effective width is modeled with a random variable, it has influence on the moment of inertia of the beam and also on the moment–rotation relationship of the plastic hinge of the beam.

Once the set of structural models is obtained, the single-record IDA curves can be calculated for each structural model from the set of structural models, and for each GMR from the set of GMR. The total number of all single-record IDA curves is therefore now $N_{\mathrm{Gmr}} \cdot N_{\mathrm{Sim}}$, where N_{Gmr} is the number of GMR used in the set of GMR and N_{Sim} is the number of structural models in the set of structural models. The results based on extended IDA analysis can be used for performance evaluation taking into account the record-to-record variability and epistemic uncertainty for the determination of the probability of exceedance of a given limit state.

In addition to IDA curves, which are the primary result of the extended IDA analysis, the importance of the effect of the input random variables on the selected EDP can also be determined.

DOI: 10.1002/eqe

Since the determination of the set of structural models is based on the LHS method, the simple approach to determine the sensitivity of the EDP to the input random variables, which has been used and explained more in greater detail elsewhere [20, 21], is based on the Spearman rank-order correlation coefficient ρ, which for the ith input random variable, is defined as

$$\rho_i = 1 - \frac{6\sum_{j=1}^{N_{\text{Sim}}} (r(x_{j,i}) - r(\text{EDP}_j))^2}{N_{\text{Sim}}(N_{\text{Sim}}^2 - 1)} \tag{4}$$

where $x_{j,i}$ is the value of the random variable X_i for the jth simulation, taken from the optimized sample matrix $\mathbf{X}$, EDP_j is the EDP for the jth simulation, e.g. maximum storey drift, top displacement, an IM corresponding to a given limit state, or other, N_{Sim} is the number of structural models used in the extended IDA analysis, and r denotes the rank of the jth sample value of the input random variable or response variable EDP. The parameter ρ may assume values between 1 and -1. If ρ has value close to 1 it means that the response variable EDP has a strong positive dependence on the selected input random variable, or vice versa, if ρ is close to -1. On the other hand, the input random variable does not have an influence on the response variable when ρ has a value close to 0.

3. CASE STUDY: A FOUR-STOREY-REINFORCED CONCRETE FRAME

3.1. Description of the structure

Extended IDA analysis was applied to a four-storey plane RC frame, which had been designed to reproduce the design practice in southern European countries about forty to fifty years ago [22]. However, it can also be typical for buildings built more recently, but without the application of capacity design principles (especially the strong column—weak beam concept), and without up-to-date detailing. The elevation, plan and typical reinforcement in the columns are presented in Figure 3. The reinforcement is reduced in the top two stories in columns B and C. In column B only three ϕ12 mm bars are placed on each of the long sides of the column. Such a configuration results in 6ϕ12 mm bars in the cross-section of column B. For column C, in the top two stories only 4ϕ16 mm bars are used in the corners of the cross-section, whereas the same reinforcement (2ϕ12 mm bars) is used in the middle of the long side of the cross-section.

All the beams are 0.25 m wide and 0.50 m deep. The bottom longitudinal reinforcement in the beams consists of 2ϕ12 mm bars. Three ϕ12 mm bars are used for the top longitudinal reinforcement at the connection to column A (Figure 3). The top reinforcement in the beams connected to column B and column D amounts to 2ϕ12+2ϕ16 mm bars. Beams, connected from both sides to column C, have the strongest reinforcement at the top of the beam (2ϕ12+5ϕ16 mm bars). The slabs are 0.15 m thick and reinforced with ϕ8/10 cm.

The design base shear coefficient amounted to 0.08. In the design, concrete of quality C16/20 and smooth steel bars of class Fe B22k (according to Italian standards) were adopted [22]. The mean strength of the concrete amounted to 16 MPa and the mean yield strength of the steel amounted to 343.4 MPa. The structure was also pseudo-dynamically tested at full scale at the ELSA Laboratory. The results of the experiments can be found in the ECOEST2-ICONS Report No. 2 [22].

DOI: 10.1002/eqe

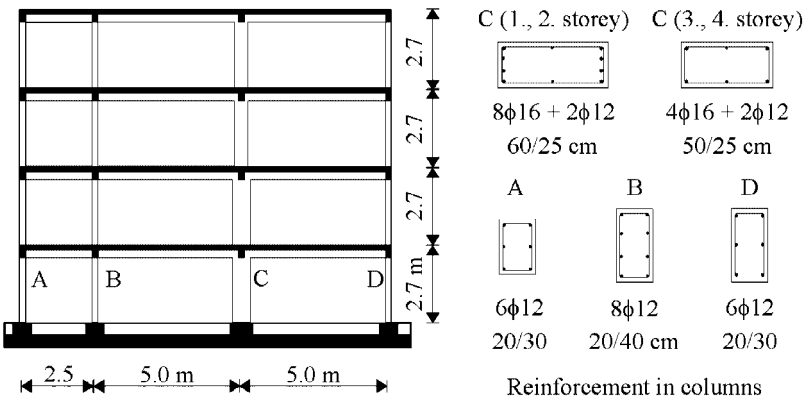

Figure 3. View and typical reinforcement of the columns of the structure.

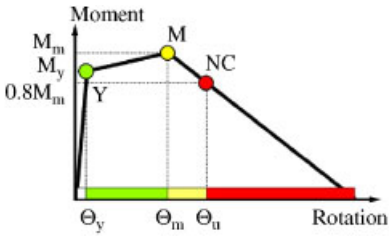

Figure 4. Schematic moment–rotation relationship of a plastic hinge (Y-yield, M-maximum, NC-near collapse).

3.2. The deterministic model

The model of the structure consisted of one-component lumped plasticity elements, which were used for modeling the beams and columns. The schematic moment–rotation envelopes of the inelastic rotational hinges are shown in Figure 4. The yield and the maximum moment in the columns were calculated taking into account the axial forces due to the vertical loading on the frame, which amounted to 9.1 and 8.0 kN/m^2 for the bottom three stories and for the top storey, respectively. Potential reduction in flexural strength due to insufficient anchorage length of the reinforcing bars was not considered when determining the moment–rotation envelopes. The effective beam width of 75 and 125 cm were determined according to the Eurocode 2 procedure [23] for the short and long beams, respectively.

The characteristic rotations, which describe the moment–rotation envelope of a plastic hinge, were determined according to the procedure described by Fajfar *et al.* [24]. The zero moment point was assumed to be at the mid-span of the columns and beams. The ultimate rotation Θ_u in the columns at the near collapse (NC) limit state, which corresponds to a 20% reduction in the maximum moment, was estimated by means of the conditional average estimate method [25]. For the beams, the EC8-3 [26] formulas were used, the parameter γ_{el} being assumed to be equal to 1.0. Owing to the absence of seismic detailing, the ultimate rotations of beams were multiplied by a factor of 0.85 [26].

DOI: 10.1002/eqe

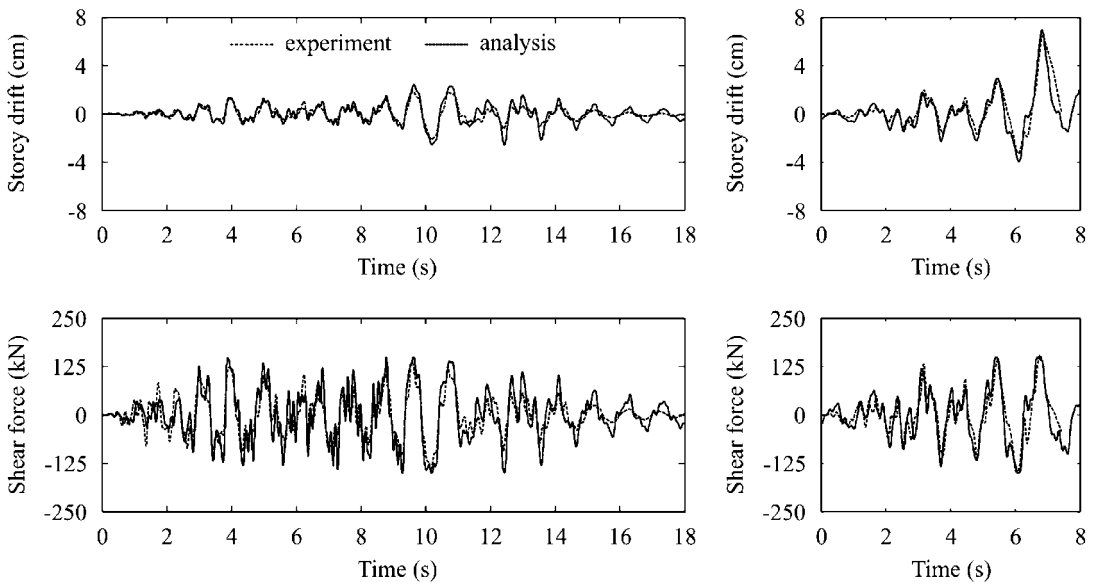

Figure 5. The calculated time histories for drift and shear force in the critical third storey, compared with the experimental results.

The deterministic model was validated by comparing the results of nonlinear dynamic analysis with the experimental results obtained in pseudo-dynamic tests [22]. The input GMR was supposed to be representative for a moderate to high European seismic hazard scenario. Two tests were performed in a series, assuming the same ground motion. The peak ground acceleration amounted to $0.22g$ and $0.29g$, respectively, for the first and second test. Comparisons between the calculated and experimental time histories for drift and shear force in the critical third storey are presented in Figure 5. Very good correlation between the calculated and test results can be observed. It can be also observed that the second test was stopped after 7 s since imminent collapse was attained at the third storey [22], which is properly simulated by means of nonlinear dynamic analysis, which was performed by OpenSees [27].

3.3. Input random variables, statistical correlation and sampling

The sources of uncertainty, which is assumed in this study, were: mass, strength of the concrete and the reinforcing steel, effective slab width, damping, and the model for determining the initial stiffness and ultimate rotation in the plastic hinges of the beams and columns. Mass was the only source of uncertainty, which was modeled with more than one random variable, since it was assumed that it can vary from storey to storey. All the input random variables considered for the determination of the set of structural models were assumed to be uncorrelated. The statistical characteristics of the input random variables are presented in Table I. A normal distribution was assumed for the majority of the random variables. The exception is the strength of the reinforcing steel, for which a lognormal distribution was assumed as recommended in the Probabilistic Model Code [30] and the random variables that model the uncertainty in prediction of the initial stiffness

DOI: 10.1002/eqe

Table I. The statistical characteristics of the input random variables.

Name		Mean or Median	COV	Distribution	Reference
Mass first storey	m_1	46 t	0.1	Normal	Ellingwood *et al.* [28],
Mass second storey	m_2	46 t	0.1	Normal	Haselton [15]
Mass third storey	m_3	46 t	0.1	Normal	
Mass fourth storey	m_4	40 t	0.1	Normal	
Concrete strength	f_{cm}	16 MPa	0.2	Normal	Melchers [29]
Steel strength	f_y	343.6 MPa	0.05	Lognormal	Melchers [29], JCSS [30]
Effective slab width	b_{eff}	75 or 125 cm	0.2	Normal	Ellingwood *et al.* [28] Haselton [15]
Damping	ξ	2	0.4	Normal	Porter *et al.* [14]
Initial stiffness of the columns	$\Theta_{y,c}$	1 computed	0.36	Lognormal	Panagiotakos and Fardis [31]
Initial stiffness of the beams	$\Theta_{y,b}$	1 computed	0.36	Lognormal	
Ultimate rotation of the columns	$\Theta_{u,c}$	1 computed	0.4	Lognormal	Peruš *et al.* [25]
Ultimate rotation of the beams	$\Theta_{u,b}$	1 computed	0.6	Lognormal	Panagiotakos and Fardis [31]

and ultimate rotation of columns and beams. The mean/median values of the random variables correspond to the best estimates employed in the deterministic model.

The coefficients of variation were taken from the literature and are presented in Table I. The highest value (0.6) was adopted for the prediction of the ultimate rotations in the beams. This is a rounded value of that reported by Panagiotakos and Fardis [31]: 0.64. A smaller value (0.4) was used for the coefficient of variation of the ultimate rotation in the columns. This is the consequence of the more reliable model that was used to determine the ultimate rotation of the columns [25]. Quite high a value for the coefficient of variation was also adopted for the initial stiffness of the beams and columns [31], and for the damping [14], which was modeled as being proportional to the tangent stiffness. For the sake of brevity, discussion regarding the dispersion of the other input random variables has been omitted, since the coefficient of variation is substantially smaller [15, 28, 29] than those described above.

The random variables were then sampled for different selected N_{Sim} values. There are two reasons for doing so. First, in general it is not known in advance which size of sample is appropriate for further analysis and second, it is important to know how much the N_{Sim} influences the EDPs. This influence will be discussed later. However, the appropriate size of the sample N_{Sim}, which is equal to the size of the set of structural models, can be based on the acceptable norm E (Equation (2)). When the norm E is reasonably low, it is assumed that the sample of random variables is appropriate. The norm E, which is calculated on the basis of the optimized sample matrix (Section 2) for different sizes of the sample N_{Sim}, and the maximum difference between the generated and prescribed correlation coefficients (E_{max}) are presented in Table II. From the results presented in Table II it can be concluded that, as expected, both norms decrease if N_{Sim} increases. However, it is more important to observe that after N_{Sim} exceeds the number of random variables N_{Var}, which is in our case equal to 12, both norms are substantially reduced. For example, if $N_{Sim} = 10$ the maximum difference between the generated and prescribed correlation coefficients

DOI: 10.1002/eqe

Table II. The norm E (Equation (2)) and the maximum difference between the generated ($S_{j,i}$) and prescribed ($K_{j,i}$) correlation coefficients for the random variables X_i and X_j, presented for different sample sizes N_{Sim}.

N_{Sim}	5	10	15	20	25	30	50
E	0.0526	0.0216	0.0020	0.0011	0.0006	0.0004	0.0001
$E_{\max}=\max(S_{j,i}-K_{j,i})$	0.9260	0.3532	0.0371	0.0225	0.0141	0.0069	0.0024

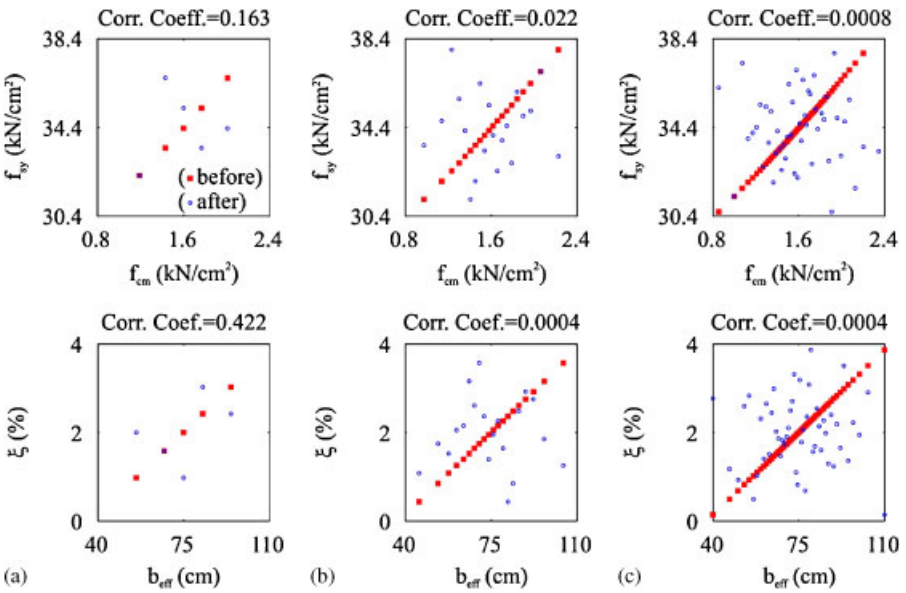

Figure 6. Comparison between the sample values of the selected random variables (concrete strength versus yield strength of the reinforcement, and beam effective width versus damping) before and after the optimization of the sample matrix **X**. The comparison has been made for different sizes of the sample (N_{Sim}): (a) $N_{\text{Sim}}=5$; (b) $N_{\text{Sim}}=20$; and (c) $N_{\text{Sim}}=50$.

$E_{\max}$ is still high (0.35), but in the case when $N_{\text{Sim}}=15$, the same norm is reduced to 0.037. Based on these results it was concluded that for this example an N_{Sim} equal to or greater than 15 is appropriate for extended IDA analysis.

The influence of the sample size N_{Sim} on the prescribed correlation can also be visually presented as shown in Figure 6. The sample values before and after the optimization of the sample matrix **X** (Section 2) are presented for two selected pairs of random variables (concrete strength versus steel strength and effective slab width versus damping). It can be observed that after optimization of the sample matrix, and if N_{Sim} exceeds N_{Var}, the correlation between the random variables is practically 0, as prescribed. Note that the method is not limited only to the uncorrelated random variables used in this example.

DOI: 10.1002/eqe

3.4. The set of GMR

The set of GMR consisted of 14 recorded GMR (Table III), which were selected from the European Strong Motion Database [32]. The acceleration spectra for each GMR and the mean spectrum are presented in Figure 7. All the records were recorded on stiff soil, and the peak ground accelerations exceeded $0.1g$. Since there are few strong GMR available in the database [32], these were the only criteria for the selection of the set of GMR, which was also employed in the previous study [33]. This set of GMR therefore may not have been sufficient for the site-specific uniform hazard spectrum, which, however, was not the primary goal of this study.

Table III. The set of ground motion records selected from the EESD [32].

Earthquake	ID	Ground motion records	$a_g(g)$
Montenegro 1979	196x	Petrovac NS	0.45
	196y	Petrovac EW	0.31
	197x	Ulcinj-Olimpic NS	0.29
	197y	Ulcinj-Olimpic EW	0.24
	199x	Bar NS	0.38
	199y	Bar EW	0.36
Campano Lucano 1980	291y	Calitri NS	0.16
	291x	Calitri EW	0.18
Kalamata1986	413x	Kalamata-Pre. N265	0.21
	413y	Kalamata-Pre. N355	0.30
	414x	Kalamata-OTE N80E	0.24
	414y	Kalamata-OTE N10W	0.27
Umbro-March. 1997	612x	Colfiorito NS	0.12
	612y	Colfiorito EW	0.11

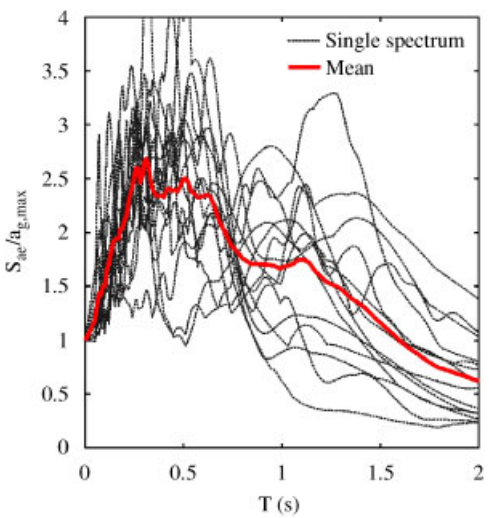

Figure 7. The elastic response spectra for 5% damping.

DOI: 10.1002/eqe

3.5. The sets of structural models

Different sets of structural models were created aimed at studying the influence of sample size (N_{Sim}) and that of the different random variables on the EDPs. First, different sets of structural models were created taking into account different sample sizes ($N_{\mathrm{Sim}}=5, 10, 15, 20, 25, 30, 50$). In this case only selected random variables, i.e. mass, concrete and steel strength, effective slab width and damping (Table I), were considered in the analysis. The IDA curves for these sets of structural models were calculated only for two GMR. The results of this study are presented in the next section. Finally, two sets of structural models were used for extended IDA analysis considering all the GMR defined in the set of GMR. In this case both sets consisted of 20 structural models ($N_{\mathrm{Sim}}=20$). However, in the first set only the selected random variables were assumed as sources of uncertainty, as explained above, whereas in the case of the second set of structural models all the random variables presented in Table I were considered as sources of uncertainty. The results of the extended IDA analysis for these sets of structural models are presented in Section 3.7.

Note that some of the other parameters of the structural models, such as elastic modulus, gravity loads, the axial forces in the columns, used for determination of the moment–rotation relationships of the plastic hinges, were linked to the appropriate random variables. For example, the elastic modulus was assumed to depend on the concrete strength according to the Eurocode 2 provisions [23], and the gravity loads and axial forces were assumed to be proportional to mass, which is considered as a random variable (Table I).

3.6. The influence of the number of structural models (N_{Sim}) on EDPs

In this section, the IDA curves for the given GMR are presented for the different sets of structural models, together with the summarized IDA curves (16, 50 and 84% fractiles) and collapse points, which correspond to global dynamic instability. The sets of structural models were determined by assuming different sample sizes N_{Sim}, as explained in the previous section. The IDA curves, which were calculated for the GMR $197y$ and $291x$, are presented in Figures 8 and 9, respectively. It can be observed that the summarized IDA curves for low N_{Sim} values (5 or 10) differ from the summarized IDA curves for higher N_{Sim} values. However, the results for the higher N_{Sim} values are stable. This can also be concluded from the results presented in Table IV, where the influence of the number of structural models (N_{Sim}) on the median peak ground acceleration ($a_{\mathrm{g,C}}$), median maximum drift, and median top displacement, all calculated based on the collapse points (see Figures 8 and 9), is presented. In addition, the dispersion measure, calculated as explained later in Section 3.8, is presented for each quantity, as well as the difference Δ between the quantity determined on the basis of the selected number N_{Sim} and the quantity determined by assuming $N_{\mathrm{Sim}}=50$, which is, in our case, the most precise result of this analysis.

It can be observed that the influence of N_{Sim} on the median $a_{\mathrm{g,C}}$ is negligible also in the case when $N_{\mathrm{Sim}}=5$. The influence of N_{Sim} on the EDPs, such as the maximum drift and top displacement, is slightly greater than that observed in the case of peak ground acceleration. However, increasing N_{Sim} does not substantially change the results. The dispersion measures, which are also presented in Table IV for the median $a_{\mathrm{g,C}}$ and both of the EDPs, also do not differ significantly for different N_{Sim} values. If the observed dispersion is low (within value of 0.1) then the relative difference in the dispersion, calculated based on an analysis with different N_{Sim} values, can be high. However, if $N_{\mathrm{Sim}} > N_{\mathrm{Var}}$, the absolute difference in the dispersion measure is low and almost always in the range ± 0.03. This is practically negligible in comparison with the difference in the dispersion measures if the results are compared for the different GMR used in this study. It can happen, as

DOI: 10.1002/eqe

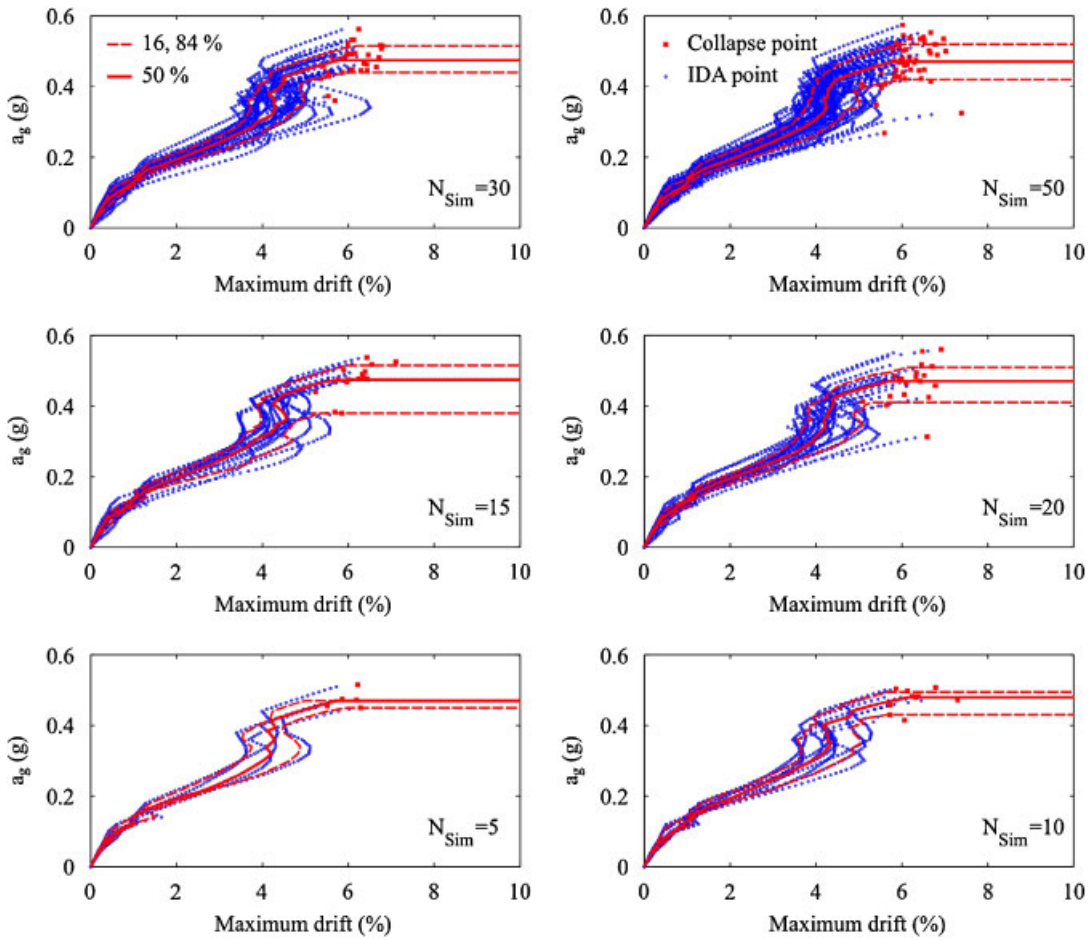

Figure 8. The summarized IDA curves (16, 50 and 84% fractiles) for maximum drift versus peak ground acceleration, the calculated IDA points, and the collapse points for ground motion 197y, for different sizes of the set of structural models (N_{Sim}).

in the case of the top displacement, that the difference in the dispersion measure for comparing the results for ground motions 197y and 291x is more than 0.3 (Table IV).

The set of structural models, which consisted of 20 structural models ($N_{\text{Sim}}=20$), was selected based on this study for further analysis, since increasing the number of structural models does not significantly influence the results. Note that for different examples, the selected size ($N_{\text{Sim}}=20$) of the set of structural models may not be appropriate.

3.7. Extended IDA analysis for two sets of structural models ($N_{\text{Sim}}=20$) and for all the GMR

Extended IDA analysis was performed for two sets of structural models, each consisting of 20 structural models ($N_{\text{Sim}}=20$), and for all the GMR defined by the set of GMR (Section 3.4). The

DOI: 10.1002/eqe

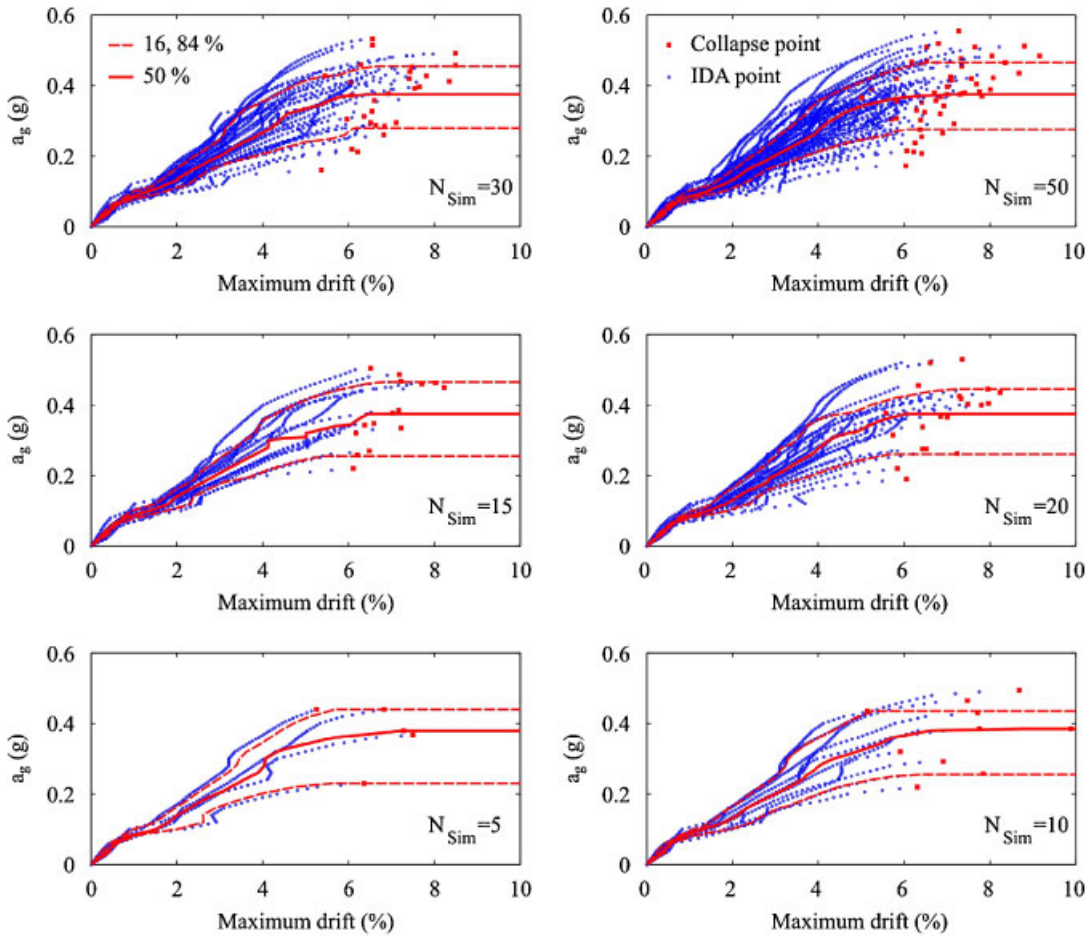

Figure 9. The summarized IDA curves (16, 50 and 84% fractiles) for maximum drift versus peak ground acceleration, the calculated IDA points, and the collapse points for ground motion 291x, for different sizes of the set of structural models (N_{Sim}).

first set of structural models was determined only from the selected random variables, whereas all of the defined random variables were employed to determine the second set of structural models (Section 3.5). The IDA curves for each structural model and for each GMR were determined by IDA [1]. The peak ground acceleration and maximum drift were defined for the IM and EDP, respectively. A hunt and fill tracing algorithm was used to calculate the IDA curves. The peak ground acceleration, which corresponds to dynamic instability, was determined with a tolerance of 0.005g. Peak ground acceleration was selected for the IM in order to simplify the presented example. The spectral acceleration corresponding to the structure's first mode period could be a better IM, but it is not a trivial IM for this example since the period of the structure differs from model to model.

DOI: 10.1002/eqe

Table IV. The influence of the number of structural models (N_{Sim}) on the median peak ground acceleration ($a_{g,C}$), the median maximum drift (*Drift*), the median top displacement (*Disp.*), all calculated based on the collapse points presented in Figures 8 and 9, the corresponding dispersion measures (β) and the absolute difference Δ between the results based on $N_{Sim}=50$ and results based on selected N_{Sim}.

N_{Sim}	$a_{g,C}$ (g)	Δ (g)	$\beta_{ag,C}$	Δ	Drift (%)	Δ (%)	β_{Drift}	Δ	Disp. (cm)	Δ (cm)	$\beta_{Disp.}$	Δ
Ground motion record: 197*y*												
5	0.473	−0.001	0.05	−0.06	6.2	0.1	0.06	−0.01	40.8	0.3	0.05	0.00
10	0.481	0.007	0.08	−0.03	6.2	0.1	0.08	0.01	41.1	0.7	0.06	0.01
15	0.478	0.004	0.09	−0.02	6.2	0.2	0.06	−0.01	41.0	0.6	0.05	0.00
20	0.474	0.0	0.10	−0.01	6.3	0.3	0.08	0.01	41.3	0.8	0.07	0.01
25	0.465	−0.009	0.08	−0.03	6.0	0.0	0.09	0.02	40.7	0.3	0.05	0.00
30	0.479	0.005	0.08	−0.03	6.1	0.0	0.08	0.02	40.6	0.2	0.06	0.00
50	0.474		0.11		6.1		0.07		40.4		0.05	
Ground motion record: 291*x*												
5	0.380	0.001	0.24	−0.02	6.8	0.0	0.14	0.02	33.6	2.4	0.27	−0.10
10	0.385	0.006	0.29	0.03	7.6	0.7	0.19	0.06	33.2	2.0	0.34	−0.03
15	0.378	−0.001	0.28	0.02	7.0	0.2	0.11	−0.01	29.1	−2.2	0.41	0.03
20	0.389	0.01	0.25	−0.01	6.9	0.1	0.14	0.01	32.1	0.9	0.35	−0.02
25	0.380	0.001	0.29	0.04	6.8	−0.1	0.14	0.01	32.8	1.6	0.39	0.02
30	0.385	0.006	0.24	−0.02	6.7	−0.1	0.15	0.03	33.4	2.2	0.38	0.00
50	0.379		0.26		6.9		0.12		31.2		0.37	

The results are presented for two ground motion records. $\Delta = X(N_{Sim}) - X(N_{Sim}=50)$.

In addition, IDA was performed for the deterministic model (Section 3.2). In this case, only the aleatory uncertainty due to the record-to-record variability was captured. The results are presented in Figure 10(a), where the summarized IDA curves are shown together with collapse points and the calculated IDA points for different peak ground accelerations and GMR.

Comparisons between the summarized IDA curves (Figure 10(a)) and the summarized IDA curves of extended IDA analysis are presented, for both sets of structural models, in Figure 10(b). Based on these results, it can be observed that the summarized IDA curves of the extended IDA analysis practically do not deviate from the summarized IDA curves, which are determined by employing the deterministic model. This observation is valid mostly for the 84% fractile curves and for the other curves within a limited range of peak ground acceleration. This is an interesting result, which leads to the conclusion, at least for the presented example, that the epistemic uncertainties do not significantly influence the summarized seismic response parameters, at least in the range NC. However, median collapse capacity is reduced for this particular example if uncertainties (see Table I) are considered in the analysis.

For a better representation of the results of the extended IDA analysis, all the calculated IDA points are presented together with the collapse points and the summarized IDA curves in Figure 10(c) and (d). The results presented in Figure 10(c) are based on a set of structural models that was created considering only selected random variables (Section 3.5), whereas the results in Figure 10(d) are based on a set of structural models for which all the random variables presented in Table I were employed in the analysis. Although there is no significant difference between the two types of summarized IDA curves, substantially higher scatter can be observed in the

DOI: 10.1002/eqe

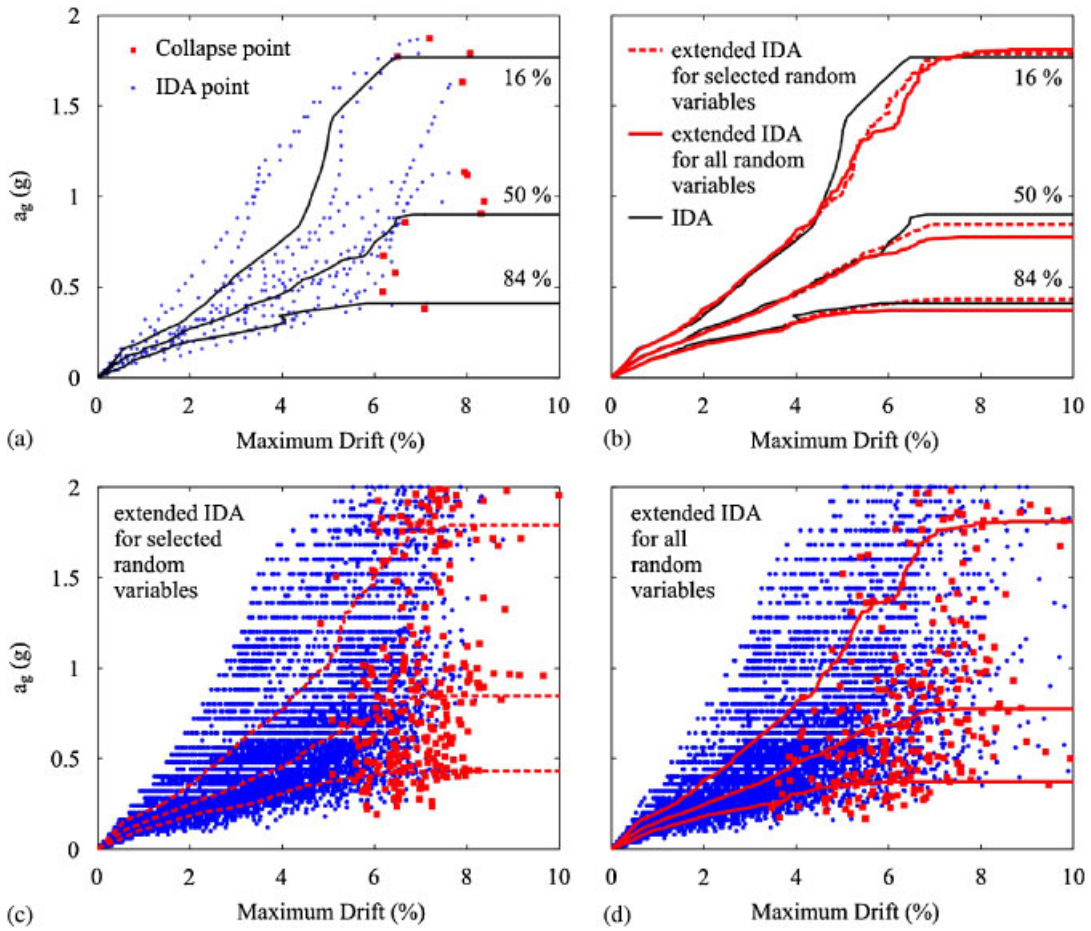

Figure 10. (a) The summarized IDA curves, collapse and IDA points for IDA analysis based on the deterministic model; (b) comparison between the summarized IDA curves and the summarized IDA curves of the extended IDA analysis for the two sets of structural models; (c) the summarized IDA curves, IDA points and collapse points of the extended IDA analysis for the set of structural models based on the selected random variables; and (d) the summarized IDA curves, IDA points and collapse points of extended IDA analysis for the set of structural models based on all the random variables.

case of the IDA points, and especially for the collapse points if the results of the extended IDA analysis (Figure 10(c) and (d)) are compared with the results of the IDA analysis (Figure 10(a)). In the case of extended IDA analysis for all the random variables (Figure 10(d)), the scatter in the collapse points is higher than the scatter in the collapse points from the extended IDA analysis for selected random variables (Figure 10(c)). This result was expected since, in the first case, the random variables, which have a high coefficient of variation, were not considered in the analysis. This difference is quantified with the dispersion measure as explained in next section.

DOI: 10.1002/eqe

3.8. Dispersion measures and the sensitivity of $a_{g,C}$ to random variables

An important result of extended IDA analysis consists of the dispersion measures and the sensitivity of the seismic response parameters (e.g. EDPs, IMs corresponding to different limit states) to the input random variables used in the analysis. The dispersion measures that are presented here were calculated based on the collapse points obtained from the extended IDA analysis for the selected random variables (Figure 10(c)) and for all the random variables (Figure 10(d)). A distinction is made between the IM-based and EDP-based dispersion measures. In the first case the dispersion (β_{agC}) was calculated for the peak ground acceleration $a_{g,C}$, which corresponds to the collapse points in Figure 10(c) and (d), whereas in the second case the dispersions are determined for the drift capacity (β_C) (collapse points in Figure 10(c) and (d)) and drift demand (β_D). Here only the dispersion for drift demand, which corresponds to the IM at the collapse point of the 84% fractile curve, is presented. This simplification enables straightforward determination of the dispersion measure for drift demand from the summarized IDA curves.

In all cases dispersion was defined as the standard deviation of the natural logarithm, which was calculated as the average value of the $\beta_{16} = \log(y_{50}/y_{16})$ and $\beta_{84} = \log(y_{84}/y_{50})$, where y_{16}, y_{50}, y_{84} represent the counted 16, 50 and 84% fractile in terms of drift demand, drift capacity or peak ground acceleration, corresponding to the drift capacity.

The extended IDA analysis makes it possible to determine the dispersion measures that reflect randomness and uncertainty (RU), and also the dispersion measures which are caused only by the uncertainties (U). In the latter case, the dispersion measures are calculated on the basis of IDA curves for the different structural models given the GMR. They therefore differ from record-to-record. However, the dispersion measures due to uncertainty, presented here, are mean values of the dispersion measures for different GMR. These dispersion measures are compared with the dispersion measure due to randomness (R), which is calculated from the IDA analysis (Figure 10(a)). All the described dispersion measures are presented in Table V. Note that terminology for the dispersion measures was adopted according to Cornell *et al.* [34] and also employed in [35]. In this case the randomness is equivalent to the aleatory uncertainty, and the uncertainty points only the epistemic uncertainty.

The dispersion for randomness in $a_{gC}(\beta_{agCR} = 0.68)$ exceeds the dispersion for uncertainty in $a_{gC}(\beta_{agCU})$. Although the dispersion for uncertainty in a_{gC} determined from the results of extended IDA analysis for all random variables ($\beta_{agCU} = 0.52$) is about twice the size of the dispersion

Table V. The dispersion measures due to randomness (β_{agCR}, β_{CR}, β_{DR}) determined from IDA analysis and the dispersion measures due to uncertainty (β_{agCU}, β_{CU}, β_{DU}) and due to both randomness and uncertainty (β_{agCRU}, β_{CRU}, β_{DRU}) determined based on extended IDA analysis for the selected and for all the random variables.

IM-based			EDP-based					
Peak ground acceleration (a_g)			Drift capacity (C)			Drift demand (D)		
β_{agCR}	0.68		β_{CR}	0.13		β_{DR}	0.46	
R. var.	Selected	All	R. var.	Selected	All	R. var.	Selected	All
β_{agCU}	0.28	0.52	β_{CU}	0.14	0.29	β_{DU}	0.22	0.29
β_{agCRU}	0.71	0.79	β_{CRU}	0.13	0.29	β_{DRU}	0.56	0.56

DOI: 10.1002/eqe

for uncertainty in a_{gC} determined from the results of extended IDA analysis for selected random variables ($\beta_{agCU}=0.28$), the difference is not reflected in the dispersion for randomness and uncertainty (β_{agCRU}), which is equal to 0.71 and 0.79, respectively, for selected and all random variables employed in the extended IDA analysis (Table V).

Significant influence of the uncertainties on the dispersion for randomness and uncertainty can be observed only in the case of drift capacity. This is the only case where the dispersion for randomness ($\beta_{CR}=0.13$) is less than the dispersion for uncertainty ($\beta_{CU}=0.14$), if the latter dispersion is based on the results of extended IDA analysis for all GMR. It can be concluded that the uncertainties in the prediction of the ultimate and yield rotation in the plastic hinges of the columns and beams have an important influence on the seismic response of the test structure.

The dispersion for randomness in the drift demand β_{DR} is 0.46, which is very close to the suggested value from previous study [35], where it was defined as 0.4 for buildings with moderate and long predominant periods. Different sets of structural models do not have an influence on the dispersion for randomness and uncertainty in the drift demand β_{DRU}, which is, in both cases, the same (0.56).

Note that the total dispersion, which reflects randomness and uncertainty (RU), can be well approximated by the square root of the sum of the squares of the dispersion measures due to randomness (R) and uncertainty (U). This is the so-called mean estimate approach, which is used and described elsewhere [19, 34] and explains the above findings that the dispersion due to uncertainty is significant when it is large relative to the dispersion due to randomness.

The sensitivity of a_{gC} to the random variables is shown in Figure 11. Since the LHS technique was used for determination of the set of structural models, the sensitivity is measured in terms of a Spearman rank correlation coefficient (Equation (4)), which is calculated here based on the extended IDA analysis for all the random variables. The results are presented for the median value of the Spearman rank correlation coefficient (horizontal line) and also for each GMR (bar). Uncertainty in damping and in the ultimate and yield rotation in the columns has the greatest influence on the a_{gC}. As expected, the former uncertainties are positively correlated with a_{gC}. The uncertainties that influence the beams are not so important, since the collapse of this structure is governed by the collapse of the columns. Other random variables, such as masses and material strength, have only a minor influence on a_{gC}, as also observed and discussed elsewhere [15, 16, 36]. However, uncertainty in strength may be important if it is considered spatially distributed, since it can cause strength irregularities in the structure [37], what was not considered in the presented example. For some random variables it is not possible to conclude whether they are positively or

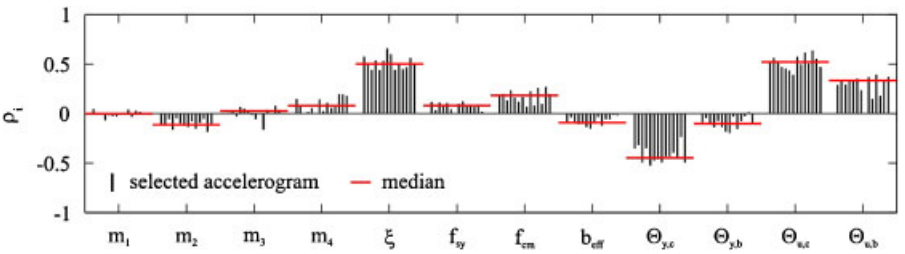

Figure 11. The Spearman rank correlation coefficient for the different random variables presented in Table II.

DOI: 10.1002/eqe

negatively correlated with the output random variable. For example, storey masses (Figure 11) can be positively or negatively correlated with a_{gC}.

4. CONCLUSIONS

The popular IDA method has been extended by introducing a set of structural models, which reflect the epistemic uncertainties. The set of structural models is determined by using the LHS method. The results of extended IDA consist of IDA curves, which capture the aleatory and epistemic uncertainties. Thus the dispersion measures, which are needed for the probabilistic seismic performance evaluation of a structure, incorporate the effects of both types of uncertainty, and not just the record-to-record variability, which results from IDA.

The applicability of the proposed method has been demonstrated by means of an example of a four-storey-reinforced concrete frame. It was shown that the accuracy of the results obtained by using the proposed method depends on the size of the set of structural models (N_{Sim}), which has to be defined prior to their determination. In the case of the presented example, it was found that the input random variables are properly sampled if the size of the set of structural models (N_{Sim}) is larger than the size of the set of input random variables (N_{Var}). In this case, the norm E obtains a low value. Increasing the size of the set of structural models much beyond N_{Var} does not improve the result, since the results are stable within this range, especially if they are expressed in terms of collapse capacity ($a_{g,C}$). A similar observation was made in the case of the dispersion measures, which are needed for probabilistic performance evaluation. The absolute difference between the dispersion measures is low and almost always within the range ± 0.03, if the size of the set of structural models (N_{Sim}) is larger than the size of the set of input random variables (N_{Var}).

Based on the results obtained in the presented example, it can be concluded that epistemic uncertainty does not have a significant effect on the seismic response parameters within the range far from collapse, but that the median collapse capacity is reduced if epistemic uncertainties are taken into account in the analysis. This conclusion is, however, not a general one. From the results of the sensitivity study it was observed that the greatest effect on the response parameters has those random variables that have a high coefficient of variation and that affect the collapse mechanism. In the presented example, these random variables are related to the initial stiffness and ultimate rotation in the columns.

The increased price for the additional information that can be obtained by employing extended IDA analysis is the longer computational time. The proposed method should therefore be aimed at the development of simplified procedures for estimating the influence of epistemic uncertainty on the seismic response parameters, and, more specifically, to define the typical values of the dispersion measures of typical structural systems, which can then be incorporated into a more practical method for the probabilistic seismic performance assessment of structures. It is expected that further research could lead to improvements in the proposed method in terms of a reduction in the computational time.

ACKNOWLEDGEMENTS

The results presented in this paper are based on work supported by the Slovenian Research Agency. This support is gratefully acknowledged.

DOI: 10.1002/eqe

REFERENCES

1. Vamvatsikos D, Cornell CA. Incremental dynamic analysis. *Earthquake Engineering and Structural Dynamics* 2002; **31**:491–514.
2. Vamvatsikos D, Cornell CA. Applied incremental dynamic analysis. *Earthquake Spectra* 2004; **10**(2):523–553.
3. Zareian F, Krawinkler H. Assessment of probability of collapse and design for collapse safety. *Earthquake Engineering and Structural Dynamics* 2007; **36**:1901–1914.
4. Tagawa H, MacRae G, Lowes L. Probabilistic evaluation of seismic performance of 3-story 3D one- and two-way steel moment-frame structures. *Earthquake Engineering and Structural Dynamics* 2008; **37**:681–696.
5. Pasticier L, Amadio C, Fragiacomo M. Non-linear seismic analysis and vulnerability evaluation of a masonry building by means of the SAP2000 V.10 code. *Earthquake Engineering and Structural Dynamics* 2008; **37**: 467–485.
6. Baker JW. Probabilistic structural response assessment using vector-valued intensity measures. *Earthquake Engineering and Structural Dynamics* 2007; **36**:1861–1883.
7. Tothong P, Luco N. Probabilistic seismic demand analysis using advanced ground motion intensity measures. *Earthquake Engineering and Structural Dynamics* 2007; **36**:1837–1860.
8. Jalayer F, Franchin P, Pinto PE. A scalar damage measure for seismic reliability analysis of RC frames. *Earthquake Engineering and Structural Dynamics* 2007; **36**:2059–2079.
9. Vamvatisikos D, Cornell CA. Direct estimation of seismic demand and capacity of multi-degree of freedom systems through incremental dynamic analysis of single degree of freedom approximation. *Journal of Structural Engineering* (ASCE) 2005; **131**(4):589–599.
10. Han SW, Chopra AK. Approximate incremental dynamic analysis using the modal pushover analysis procedure. *Earthquake Engineering and Structural Dynamics* 2006; **35**:1853–1873.
11. Dolšek M, Fajfar P. Simplified probabilistic seismic performance assessment of plan-asymmetric buildings. *Earthquake Engineering and Structural Dynamics* 2007; **36**:2021–2041.
12. Azarbakht A, Dolšek M. Prediction of the median IDA curve by employing a limited number of ground motion records. *Earthquake Engineering and Structural Dynamics* 2007; **36**:2401–2421.
13. Solberg KM, Dhakal RP, Mander JB, Bradley BA. Computational and rapid expected annual loss estimation methodologies for structures. *Earthquake Engineering and Structural Dynamics* 2008; **37**:81–101.
14. Porter KA, Beck JL, Shaikhutdinov RV. Investigation of sensitivity of building loss estimates to major uncertain variables for the Van Nuys testbed, California Institute of Technology. *PEER Report 2002/2003*, Pacific Earthquake Engineering Research Center, University of California, Berkeley, August 2002.
15. Haselton CB. Assessing seismic collapse safety of modern reinforced concrete moment frame buildings. *Ph.D. Dissertation*, Stanford University, 2006.
16. Lee T-H, Mosalam KM. Seismic demand sensitivity of reinforced concrete shear-wall building using FOSM method. *Earthquake Engineering and Structural Dynamics* 2005; **34**:1719–1736.
17. Baker JW, Cornell CA. Uncertainty propagation in probabilistic seismic loss estimation. *Structural Safety* 2008; **30**:236–252.
18. Liel A, Haselton C, Deierlein G, Baker J. Assessing the seismic collapse risk of reinforced concrete frame structures, including the effects of modeling uncertainties. *Special Workshop on Risk Acceptance and Risk Communication*, Stanford University, 26–27 March 2007.
19. Liel AB, Haselton CB, Deierlein GG, Baker JW. Incorporating modeling uncertainties in the assessment of seismic collapse risk of buildings. *Structural Safety* 2008; DOI: 10.1016/j.strusafe.2008.06.002.
20. Vorechovsky M, Novak D. Statistical correlation in stratified sampling. In *ICAPS 9 Proceedings of International Conference on Applications of Statistics and Probability in Civil Engineering*, Der Kiureghian A, Madant S, Pestana JM (eds). Millpress: Rotterdam, San Francisco, 2003; 119–124.
21. Kala Z. Sensitivity analysis of the stability problems of thin-walled structures. *Journal of Constructional Steel Research* 2005; **61**:415–422.
22. Carvalho EC, Coelho E. Seismic assessment, strengthening and repair of structures. *ECOEST2-ICONS Report No. 2*, European Commission—'Training and Mobility of Researchers' Programme, 2001.
23. CEN. Eurocode 2: design of concrete structures—Part 1-1: general rules and rules for buildings. *EN 1992-1-1*, European Committee for Standardisation, Brussels, December 2004.
24. Fajfar P, Dolšek M, Marušić D, Stratan A. Pre- and post-test mathematical modelling of a plan-asymmetric reinforced concrete frame building. *Earthquake Engineering and Structural Dynamics* 2006; **35**:1359–1379.
25. Peruš I, Poljanšek K, Fajfar P. Flexural deformation capacity of rectangular RC columns determined by the CAE method. *Earthquake Engineering and Structural Dynamics* 2006; **35**:1453–1470.

26. CEN. Eurocode 8: design of structures for earthquake resistance—Part 3: strengthening and repair of buildings. *EN 1998-3*, European Committee for Standardisation, Brussels, March 2005.
27. McKenna F, Fenves GL. Open system for earthquake engineering simulation. Pacific Earthquake Engineering Research Center, Berkeley, CA. Available from: http://opensees.berkeley.edu/, 2004.
28. Ellingwood B, Galambos TV, MacGregor JG, Cornell CA. *Development of a Probability-based Load Criterion for American National Standard A58*. National Bureau of Standards, Washington, DC, 1980; 222.
29. Melchers RE. *Structural Reliability Analysis and Prediction*. Wiley: New York, 1999.
30. JCSS. *Probabilistic Model Code—Part 1*: *Basis of Design* (12th draft). Joint Committee on Structural Safety, March 2001. Available from: http://www.jcss.ethz.ch/.
31. Panagiotakos TB, Fardis MN. Deformations of reinforced concrete at yielding and ultimate. *ACI Structural Journal* 2001; **98**(2):135–147.
32. Ambraseys N, Smith P, Bernardi R, Rinaldis D, Cotton F, Berge-Thierry C. *Dissemination of European Strong-Motion Data*. CD-ROM collection. European Council, Environment and Climate Research Programme, 2000.
33. Dolšek M, Fajfar P. Inelastic spectra for infilled reinforced concrete frames. *Earthquake Engineering and Structural Dynamics* 2004; **33**(15):1395–1416.
34. Cornell CA, Jalayar F, Hamburger RO, Foutch DA. Probabilistic basis for 2000 SAC federal emergency management agency steel moment frame guidelines. *Journal of Structural Engineering* (ASCE) 2002; **128**(4): 526–533.
35. Dolšek M, Fajfar P. Simplified probabilistic seismic performance assessment of plan-asymmetric buildings. *Earthquake Engineering and Structural Dynamics* 2007; **36**:2021–2041.
36. Krawinkler H (ed.). Van Nuys hotel building testbed report: excercising seismic performance assessment. *PEER Report 05/11*, October 2005.
37. Chintanapakdee C, Chopra AK. Seismic response of vertical irregular frames: response history and modal pushover analyses. *Journal of Structural Engineering* 2004; **130**(8):1177–1185.

DOI: 10.1002/eqe